

A crystal form of PSMD10^{Gankyrin} with channels accessible to small molecules

M. G. Mukund Sudharsan and Prasanna Venkatraman*

Protein Interactome Laboratory for Structural and Functional Biology, Advanced Centre for Treatment, Research and Education in Cancer, Kharghar, Navi Mumbai 412 100, India; and Homi Bhabha National Institute, 2nd Floor, BARC Training School Complex, Anushaktinagar, Mumbai 400 094, India

New crystal forms and conditions that aid in rapid formation of crystals would ease the efforts in drug discovery. In addition, if such new crystal forms also yielded high-resolution protein structures, then they can become better templates for screening of drugs using computational tools with better outcome. Such structures are also essential for unambiguous determination of side-chain positions such that subtle conformational changes attributed to mutations, protein dynamics and interactions are true to the proposed mechanism. In this study, we have identified a buffer cocktail which enables crystallization of PSMD10^{Gankyrin} in a novel crystal form. PSMD10^{Gankyrin} is important in the biology of the proteasome assembly and functions of the ubiquitin proteasome pathway. It is also a sought-after therapeutic oncoprotein in multiple cancers. This crystal form yielded a high-resolution structure of PSMD10^{Gankyrin} solved at 1.71 Å. The protein in the crystal is relatively less densely packed with its symmetry-related neighbours. Channels seen all around the protein would guide soaked small molecules to the exposed binding sites. We show that the AlphaFold predicted model can be used as an molecular replacement ensemble to solve structures. We also highlight the differences between the current structure and the AlphaFold structure. Thus, the crystal form of PSMD10^{Gankyrin} provides novel insights and opportunities for drug discovery.

Keywords: Crystal forms, drug discovery, protein structures, small molecules.

PSMD10^{Gankyrin}, a non-ATPase component of the proteasome and a chaperone of the proteasome assembly is also an oncoprotein¹. It was originally found to be overexpressed in tumour tissues from hepatocellular carcinoma patients² and its oncogenic function was confirmed when NIH3T3 cells overexpressing PSMD10^{Gankyrin} injected into nude mice formed tumours. When PSMD10^{Gankyrin} expression is silenced, cells undergo reduced proliferation and reduced colony formation on soft agar assay^{3,4}. When PSMD10^{Gankyrin}-silenced pancreatic cancer cells were injected into nude mice, the tumours formed were of reduced

size. In contrast, when PSMD10^{Gankyrin} was overexpressed, these cells formed large-sized tumours⁵. KRAS-mediated oncogenic signalling was dependent on the presence of PSMD10^{Gankyrin} (ref. 6).

Like many well-known oncoproteins, PSMD10^{Gankyrin} decreases the level of both Rb and p53, two major tumour suppressors in human cells. By directly binding to MDM2, PSMD10^{Gankyrin} facilitates the degradation of p53 (ref. 7). By directly binding to Rb, PSMD10^{Gankyrin} increases Rb phosphorylation and degradation by the proteasome resulting in the release of E2F, a transcription factor responsible for cellular proliferation. PSMD10^{Gankyrin} is also known to interact with CDK4 kinase, which may be necessary for cell-cycle regulation⁸. By directly binding to CLIC1, PSMD10^{Gankyrin} promotes cell migration⁹. Overexpression of PSMD10^{Gankyrin} in neural progenitor cells was suggested to drive neuronal differentiation¹⁰.

The crystal structure of PSMD10^{Gankyrin} (PDB-1UOH, 1QYM) provided the first insights into the atomic structure of the bean-shaped protein formed by seven ankyrin repeats¹¹. The co-crystal structure of PSMD10^{Gankyrin} and the C-terminal region of PSMC4 (S6C) (PDB-2DVW, 3AJI) provided details of the interaction interfaces on PSMD10^{Gankyrin} (ref. 12).

The complex structure also formed the template for the identification of a hotspot region at the interface, and a short linear sequence motif (SLiM) corresponding to residues EEVD was found to be conserved in many of the interacting partners proposed and identified for PSMD10^{Gankyrin} (ref. 9). Inhibition of this interaction also led to inhibition of PSMD10^{Gankyrin}-dependent function. These results provided the impetus to find inhibitors that could block the binding surface of PSMD10^{Gankyrin}. For proteins that can be crystallized, one of the sought-after methods is crystal screening, where small molecules that could bind to the protein can be identified by simply soaking the compounds into the preformed crystal. For this approach to be successful, it is desirable to find conditions that form crystals with accessible binding pocket and provide good-quality crystals that can be solved to high resolution. With this aim we screened for multiple conditions and found an optimal buffer cocktail that allowed PSMD10^{Gankyrin} to crystallize in a new condition. The crystal formed with a significantly reduced crystallization

*For correspondence. (e-mail: vprasanna@actrec.gov.in)

Table 1. Information on production macromolecules

Source organism	Human
DNA source	Gankyrin pBluescript II SK (1) construct (kind gift from Dr Jun Fujita, Kyoto University, Japan)
Forward primer	5'-GGATCCATGGAGGGGTGTGTGTCTAACC-3'
Reverse primer	5'-GAATCTTAACCTTCCACCATTCTCTTGAG-3'
Cloning vector	pRSETA
Expression vector	pRSETA
Expression host	<i>Escherichia coli</i> Rosetta 2DE3
Complete amino acid sequence of the construct produced	MEGCVSNLMVCNLAYSGKLEELKESILA DKSLATRTDQDSRTALHWACSAGHTEIV EFLQLGVPVNDKDDAGWSPHIAASA GRDEIVKALLGKGAQVNAVQNQNGCTPL HYAASKNRHEIAVMLLEGGANPDAKDH YEATAMHRAAAKGNLKMIIHILLYKAS TNIQDTEGNTPLHLACDEERVEEAKLLV SQGASIYIENKEEKTPAQVAKGGLGLILK RMVEG

time. We have solved the structure at a higher resolution than the previously reported structure and report advantages the structure offers for drug discovery. We also show that the AlphaFold predicted structural models can serve as good molecular replacement (MR) ensembles which should truly help in situations where there are no available structures for proteins. Comparative analysis of the solved PSMD10^{Gankyrin} structure with the predicted AlphaFold model shows some differences which are described here.

Materials and methods

Macromolecule production

PSMD10^{Gankyrin} wild type (WT) was expressed as 6× His-tagged protein in *Escherichia coli* Rosetta (2DE3). One litre of LB supplemented with 100 µg ml⁻¹ ampicillin and 37 µg ml⁻¹ chloramphenicol was inoculated and grown at 37°C to OD 600 nm = 0.5. Expression of PSMD10^{Gankyrin} was induced with 100 µM IPTG and grown for 12 h at 18°C. The cells were pelleted down and resuspended in lysis buffer (50 mM Tris/Cl pH 7.5, 150 mM NaCl, 2 mM β-ME, and 1× protease inhibitor cocktail). The cells were lysed by sonication (six pulses of 60 sec for 30 min). The cell debris was removed by centrifugation at 30,000 g for 30 min at 4°C. The soluble fraction was purified by Ni-IDA chelating chromatography (Clontech, Takara, Japan). The soluble fraction was also incubated with Ni-IDA beads in a Rotospin at 8 rpm for 1 h at 4°C. The unbound fraction was collected and the column was washed thrice with 10× bead volume of lysis buffer supplemented with 10 mM imidazole. The column was further washed once with two-bed volumes of lysis buffer supplemented with 50 mM imidazole, followed by 100 mM imidazole. The protein was eluted with lysis buffer supplemented with 250 mM imidazole. The fractions containing PSMD10^{Gankyrin} were identified by SDS-PAGE, were pooled and dialysed against 50 mM Tris pH 7.5, 150 mM NaCl. The histidine

tag was removed using in-house purified TEV protease and the untagged protein was subjected to Ni-IDA affinity followed by gel filtration on a Hiload 16/600 Superdex 200 column (GE Healthcare, Chicago, IL, USA). Peak fractions were collected. Protein was concentrated using Amicon centrifugal columns (MWCO 3K), dialysed in 50 mM Tris/Cl pH 7.5, 150 mM NaCl, and finally snap frozen at -80°C in aliquots. The purity of protein preparation was confirmed by Coomassie staining. Protein concentration was determined using the Pierce BCA protein assay kit (Thermo Scientific, Waltham, MA, USA).

The thermal stability of PSMD10^{Gankyrin} WT protein was determined by monitoring the intrinsic tryptophan fluorescence using nano-DSF (Prometheus NT.48, Nano-temper Technologies, Munchen, Germany). Data were plotted using intensity ratio of tryptophan (350/330 nm) as a function of temperature. The first derivative was used to determine melting temperature (T_m) (Table 1)¹³.

Crystallization

PSMD10^{Gankyrin} WT crystallization was set up using a sitting drop plate of Art Robbins 48-well Intelliplate (Hampton Research). The crystals grew in 60% tacsimate pH 7.0 (Hampton Research) at 22°C for four days. Next, 5–20 mg ml⁻¹ protein (drop size – 1.5 µl protein + 1 µl buffer) was screened for crystallization and the crystals grew in all concentrations.

The crystallization of PSMD10^{Gankyrin} in 60% tacsimate pH 7.0 using the hanging drop method yielded needles. These needles were broken into small pieces using a crystal crusher (Hampton Research) and were used as nucleation seeds. We observed that upon supplementing the wells with the seeds, the number of crystals in the wells increased. Crystals suitable for X-ray diffraction analysis were grown by the sitting drop vapour-diffusion technique in 60% tacsimate pH 7.0 supplemented with the seeds, and the crystals grew in five days (Figure 1 c) (Table 2).

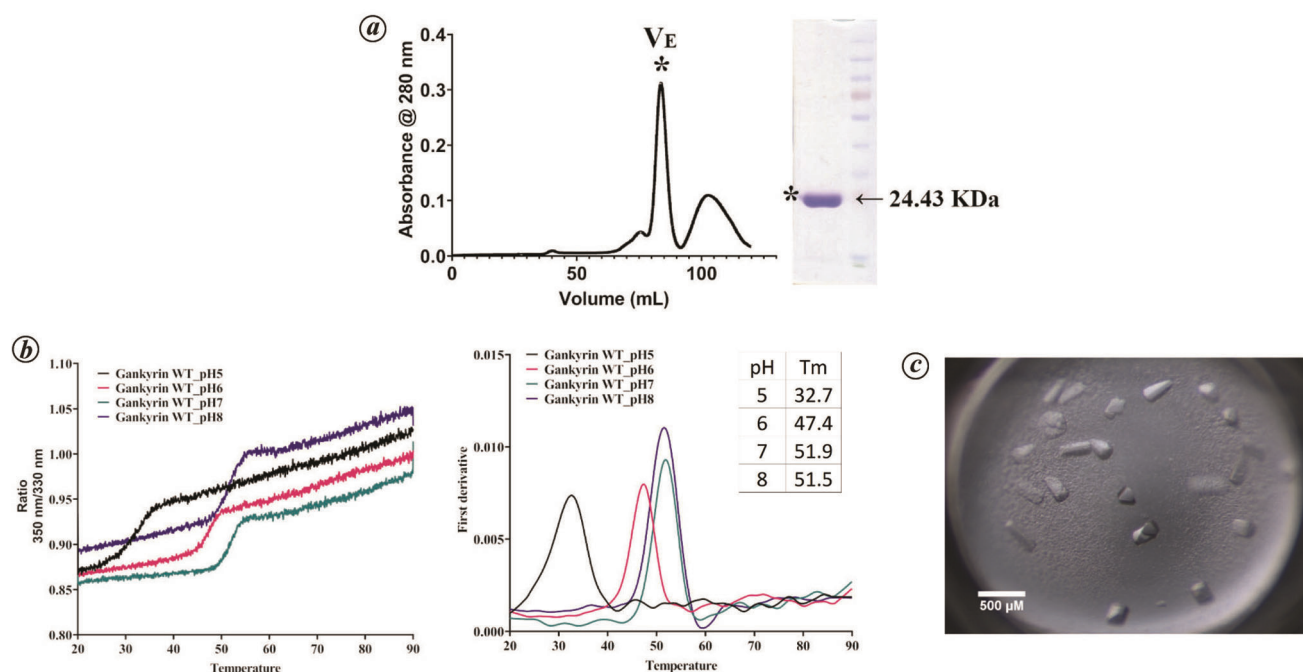


Figure 1. Purification, stability and crystals of PSMD10^{Gankyrin}. **a**, FPLC profile of PSMD10^{Gankyrin} as purified from HiLoad 16/600 Superdex 200 column and gel image depicting the purified protein. **b**, Melting temperature of PSMD10^{Gankyrin} as a function of pH measured using tryptophan fluorescence. **c**, Representative image depicting the crystals of PSMD10^{Gankyrin} used for diffraction.

Table 2. Crystallization

Method	Vapour diffusion
Plate type	Sitting drop
Temperature (K)	295
Protein concentration	20 mg/ml
Buffer composition of protein solution	50 mM Tris pH 7.5, 150 mM NaCl
Composition of reservoir solution	60% Tacsimate pH 7
Volume and ratio of drop	4 μl – buffer : protein : seed :: 1 : 2 : 1
Volume of reservoir	200 μl

Data collection and processing

Data for PSMD10^{Gankyrin} WT were collected at synchrotron beamline ($\lambda = 0.9795 \text{ \AA}$) at PX-BL21, RRCAT, Indore. Automated data reduction and scaling were performed using XIA2 in the CCP4 suite^{14,15}.

Structure solution and refinement

The structure was determined using MR with Phaser-MR in Phenix suite¹⁶. PDB entry 1UOH was used as the search model. Refinement was performed using Refmac5 in the CCP4 suite^{15,17}, and model-building was done using the program Coot¹⁸. The models for representation were made using either PYMOL or Chimera v.1.31 (refs 19, 20). Structure alignment was performed using PYMOL.

Results

Purification of PSMD10^{Gankyrin} WT and its stability

PSMD10^{Gankyrin} WT was obtained by overexpression in *E. coli* Rosetta 2DE3. The protein of crystallographic-grade purity was obtained by Ni-NTA metal-affinity followed by gel-filtration chromatography (Figure 1 a). The stability of PSMD10^{Gankyrin} in Tris buffer, pH 5–8 was determined using NanoDSF. PSMD10^{Gankyrin} WT protein was stable at pH 7 and 8 compared to pH 5 or 6 (Figure 1 b).

Updated higher-resolution crystal structure for PSMD10^{Gankyrin}

The crystals in this space group diffracted to 1.5 Å at the PX-BL21 beamline of the synchrotron facility at RRCAT, Indore. Since the number of unique reflections was small at this resolution, we used data at 1.71 Å resolution to solve the structure using the program Phaser from Phenix.

Solutions were obtained by MR using the already existing crystal structure of PSMD10^{Gankyrin} WT solved at a resolution of 2.0 Å (PDB entry – 1UOH). Although the space group was different (P3₂2₁ vis-à-vis 1UOH in P2₁2₁2₁), the structure of PSMD10^{Gankyrin} was highly similar to 1UOH (Figure 2 a). Table 3 lists the statistics for the proposed structure with the PDB ID-7VO6.

The overall structural characteristics between the previously solved PSMD10^{Gankyrin} structure and that from the

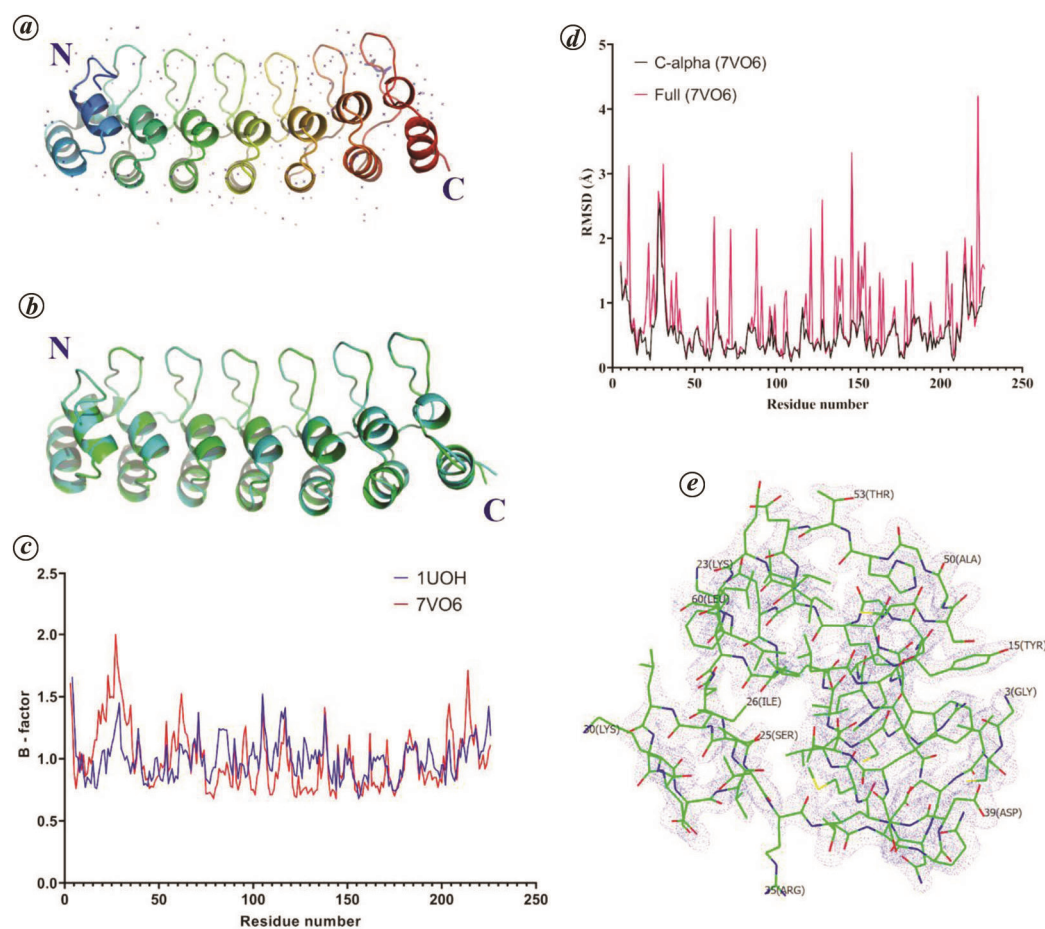


Figure 2. High-resolution structure of PSMD10^{Gankyrin} and comparative analysis. *a*, Crystal structure of PSMD10^{Gankyrin} solved at 1.71 Å (PDB ID-7VO6). *b*, Alignment of structures solved using two different search models by molecular replacement (MR) (green – 1UOH, cyan – Alphafold). *c*, Plot comparing differences in *B*-factor between 1UOH and 7VO6. *d*, Electron density of residues 3 to 60 from 7VO6 (map – blue dots) showing higher *B*-factor. *e*, Plot of *C*α RMSD between 1UOH and 7VO6.

present study (PDB ID-7VO6) are similar. Residues 3-60 in the N-terminus region display higher *B*-factor value in 7VO6 (Figure 2 *c*), despite the fact that the experimental electron density map of 7VO6 and the MR model (1UOH) fitted extremely well for these residues (Figure 2 *d*). The changes in the region of residues 3–60 are also reflected in the *C*α and per residue RMSD plots obtained by a comparison with 1UOH (Figure 2 *e*). These observations together indicate that this region is flexible and is captured in the proposed structure probably owing to the relatively less tight packing (discussed below).

MR is the most popular method of solving structures and relies on structural homology. However, for many proteins such starting structures are not yet available. For any theoretical model to be used for solving the structures, it must be highly accurate. Alphafold has revolutionized the field of structural biology with its ability to predict structural models with high precision²¹. It is potentially possible to use these models as MR ensembles and, if successful, they will be useful in the case proteins for

which no homologous structures are available²². To evaluate the usability of Alphafold models for phasing, we used the Alphafold predicted structure of PSMD10^{Gankyrin} as the search model for MR. The solved structure aligned entirely with the structure solved using 1UOH as the search model (RMSD=0.039) (Figure 2 *b*).

PSMD10^{Gankyrin} WT crystallized into a form with less dense packing and accessible channels

Under the conditions reported here, PSMD10^{Gankyrin} crystallized in a new space group (7VO6, P3₂2₁ vis-à-vis 1UOH in P2₁2₁2₁). The Matthews coefficient of 7VO6 and 1UOH is 2.55 and 1.8 Å Da⁻¹ respectively. Notably, the solvent content of 7VO6 is 51.81% compared to 32.6% in 1UOH. Both the Matthews coefficient and solvent content indicate that 1UOH crystal form has a tighter packing, while 7VO6 is relatively less tightly packed (Figure 3 *a* and *b*)²³. This organization of PSMD10^{Gankyrin}

in the new crystal form prompted us to look for channels that can lead to the protein binding sites.

We used the MAP_CHANNELS tool to obtain the map of the solvent channel and compared its characteristics in the two crystal forms²⁴. We have contoured the map at 5σ for both the crystals. While we did not observe any channel in the 1UOH structure, 7VO6 had an extensive channel system. Using the same tool, we calculated the dimensions of the channel. The 1UOH crystal had a narrow solvent channel with a radius of 1.6 Å, while 7VO6 had a wider solvent channel of radius 5.4 Å (~3.5 times wider), strikingly along all the three axes (Figure 3 c–g). The tunnel characteristics indicate that the tortuosity of 7VO6 is 2.14, indicating that the tunnel has a slight curvature

which may regulate the nature and size of the small molecules that can readily diffuse into the PSMD10^{Gankyrin} 7VO6 crystals.

Besides the aqueous channel, it is important that the binding surface of PSMD10^{Gankyrin} (any protein) is exposed in the packed crystal for successful screening of small molecules. The binding site on the curved concave surface of PSMD10^{Gankyrin} constituted by residues R41, K116 and L178–E182 were all clearly accessible, as defined by the map (Figure 3 h). We observed finger-like projections in the map reaching out to the binding surface on PSMD10^{Gankyrin}, indicating that if 7VO6 crystals are soaked in a small molecule, the latter could reach the surface of PSMD10^{Gankyrin} (Figure 3 i).

Table 3. Data collection and refinement statistics

	PSMD10 ^{Gankyrin} WT (PDB ID-7VO6)
Wavelength (Å)	0.9795
Temperature (K)	80
Detector	MARCCD225
Crystal-detector distance (mm)	170
Rotation range per image (°)	1
Total rotation range (°)	30.00–191.00
Resolution range	47.89–1.71 (1.771–1.71)
Space group	P3 ₂ 21
Unit cell	60.0846 60.0846 122.377 90 90 120
Total reflections	277,094 (26,587)
Unique reflections	28,394 (2760)
Multiplicity	9.8 (9.5)
Completeness (%)	99.82 (98.68)
Mean $I/\sigma(I)$	9.29 (0.42)
Wilson B-factor	25.73
R-merge	0.09388 (0.9905)
R-meas	0.09915 (1.047)
R-pim	0.03162 (0.336)
CC1/2	0.998 (0.819)
CC*	1 (0.949)
Reflections used in refinement	28,349 (2762)
Reflections used for R-free	1,505 (142)
R-work	0.2063 (0.3841)
R-free	0.2332 (0.3724)
CC (work)	0.960 (0.658)
CC (free)	0.953 (0.513)
Number of non-hydrogen atoms	1,912
Macromolecules	1,694
Ligands	7
Solvents	211
Protein residues	224
RMS (bonds)	0.017
RMS (angles)	1.9
Ramachandran favoured (%)	95.95
Ramachandran allowed (%)	4.05
Ramachandran outliers (%)	0
Rotamer outliers (%)	1.12
Clash score	5
Average B-factor	29.63
Macromolecules	28.38
Ligands	38.67
Solvents	39.39

Statistics for the highest resolution shell is shown in parentheses.

R-pim = $0.8 * 0.42 = 0.336$.

Discussion

PSMD10^{Gankyrin} is a well-established oncogene in multiple cancers responsible for many hallmark properties of cancer and is associated with poor prognosis in many hard-to-treat cancers^{2,25–27}. It is considered as a valuable therapeutic target. However, lacking any enzymatic activity or receptor-like binding clefts, PSMD10^{Gankyrin} has been a difficult target. Only a couple of studies have identified small molecules against PSMD10^{Gankyrin} (refs 28–30). A small molecule-bound crystal structure of PSMD10^{Gankyrin} is not available. Since the existing crystal form of PSMD10^{Gankyrin} takes too long to crystallize and is a tightly packed crystal (PDB ID-1UOH), we explored if we could get better crystals which can be used in high-throughput screening. Here, we have identified a novel crystal form with solvent channels that are amenable for small-molecule transport into the crystal upon soaking²⁴. The binding site in the proposed crystal form is also open to such incoming small molecules. These properties combined with the faster crystallization times (~5 days) present an opportunity to rapidly screen for molecules that can bind to the interface in PSMD10^{Gankyrin}, shared by few of the interacting proteins³¹. Such small molecules are highly likely to inhibit the functions of PSMD10^{Gankyrin} relying primarily on protein–protein interactions for its oncogenic activity and can act as lead compounds for drug discovery.

Our solution at 1.71 Å thus far represents the best reported resolution for the structure of PSMD10^{Gankyrin}. Therefore, we compared the crystal structure reported in this study with other PSMD10^{Gankyrin} structures. Both 7VO6 and 1UOH are the apo structures. They are highly similar, except in the region that defines the N-terminus of the protein with a higher B-factor, indicating that the N-terminal region as captured in the crystal form is flexible and dynamic. There are few residues with a RMSD >2 Å between the 1UOH and 7VO6 structures. These differences arise because some of them do not have complete densities in either structures, or some lack complete/partial density in one or the other. For example, D71,

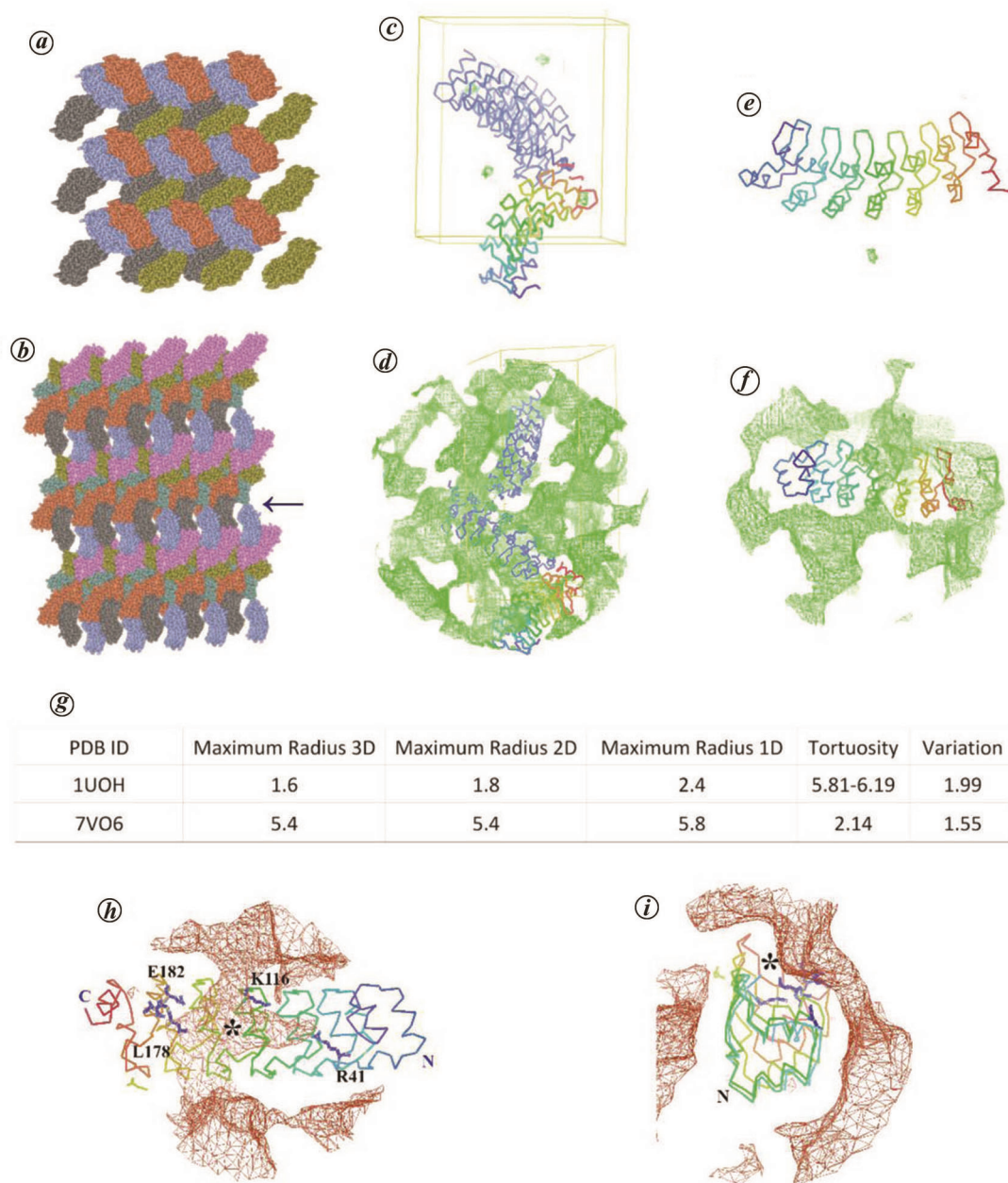


Figure 3. Crystal packing of 1UOH and 7VO6. Cell symmetry with all the symmetry molecules represented as space-fill models: (a) 1UOH and (b) 7VO6. Solvent channel maps (solid brown) through the unit cell of (c) 1UOH and (d) 7VO6. Solvent channel maps around the surface of one molecule of PSMD10^{Gankyrin} in (e) 1UOH and (f) 7VO6. g, Solvent channel properties of 1UOH and 7VO6. h, i, Accessibility of the binding site residues through solvent channels (map – brown mesh, region – *).

E127 and R145 are described by complete density in 7VO6, while in 1UOH they lack full density (Figure 2 d and Supplementary Table 1).

We also compared the AlphaFold predicted structure with 7VO6 and 1UOH (Figure 4 a). Interestingly, only a short stretch of residues 1–9 did not align with 7VO6 or 1UOH. These residues were also marked as a less confident prediction by AlphaFold, indicating that the scoring system of the AI-based prediction is realistic. In comparison with 7VO6, we observed 17 residues of AlphaFold structure

with RMSD >2 Å. Specifically, the C-terminus residues (213–215, 218–219, 222–226) differed from 7VO6 (with complete density in 7VO6) with RMSD >2 Å indicating that they take a slightly different conformation in the predicted model (Figure 4 b and c and Supplementary Table 1). These differences could be due to the inherent flexibility of this region supported by its ready melting in the crystals soaked in urea (unpublished). Simulation studies also show that unfolding of PSMD10^{Gankyrin} begins at the C-terminus³².

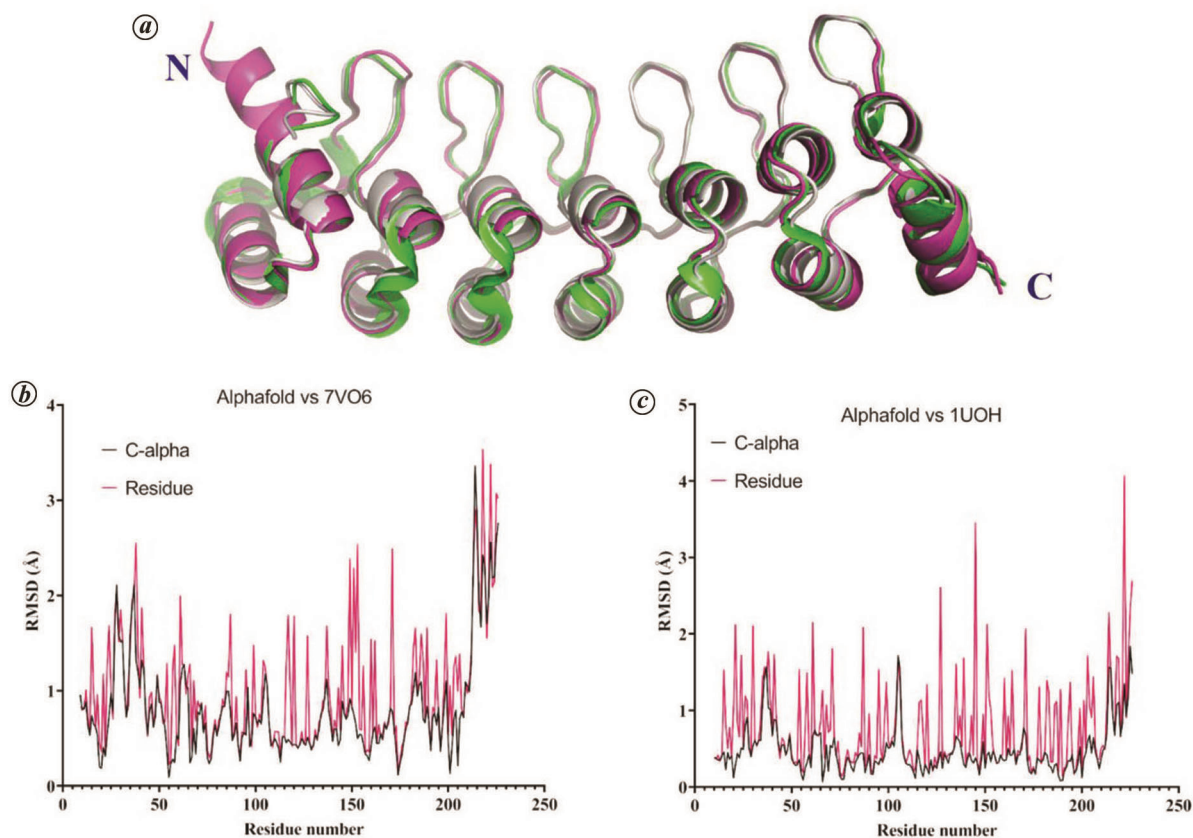


Figure 4. Comparison of different structures of PSMD10^{Gankyrin} and conformational changes in the bound form of PSMD10^{Gankyrin}. **a**, PSMD10^{Gankyrin} structures – structure from this study (PDB ID-7VO6) (cyan) and AlphaFold model (pink), all aligned to 1UOH (green). **C** α and per residue RMSD plot for **(b)** AlphaFold versus 7VO6, and **(c)** AlphaFold versus 1UOH.

In conclusion, we have obtained crystallization conditions that encourage PSMD10^{Gankyrin} to pack with sufficiently large solvent channel that can guide small molecules to its open binding site carrying functional groups. We also report that AlphaFold models are very good MR templates and can be extremely useful when there are no structures available to solve the phase problem. The present study also highlights that multiple crystal forms of the same protein and a combination of hybrid methods can be useful to determine the protein structure, dynamics and in drug development programmes.

1. Bedford, L., Paine, S., Sheppard, P. W., Mayer, R. J. and Roelofs, J., Assembly, structure, and function of the 26S proteasome. *Trends Cell Biol.*, 2010, **20**, 391–401.
2. Higashitsuji, H. *et al.*, Reduced stability of retinoblastoma protein by gankyrin, an oncogenic ankyrin-repeat protein overexpressed in hepatomas. *Nature Med.*, 2000, **6**, 96–99.
3. Fu, X. Y., Wang, H. Y., Tan, L., Liu, S. Q., Cao, H. F. and Wu, M. C., Overexpression of p28/gankyrin in human hepatocellular carcinoma and its clinical significance. *World J. Gastroenterol.*, 2002, **8**, 638–643.
4. Park, T. J., Kim, H. S., Byun, K. H., Jang, J. J., Lee, Y. S. and Lim, I. K., Sequential changes in hepatocarcinogenesis induced by diethylnitrosamine plus thioacetamide tamide in fischer 344 rats: induction of gankyrin expression in liver fibrosis, pRB degrada-

tion in cirrhosis, and methylation of p16INK4A exon 1 in hepatocellular carcinoma. *Mol. Carcinog.*, 2001, **30**, 138–150.

5. Meng, Y. *et al.*, Gankyrin promotes the proliferation of human pancreatic cancer. *Cancer Lett.*, 2010, **297**, 9–17.
6. Man, J. *et al.*, Gankyrin plays an essential role in Ras-induced tumorigenesis through regulation of the RhoA/ROCK pathway in mammalian cells. *J. Clin. Invest.*, 2010, **120**, 2829–2841.
7. Higashitsuji, H. *et al.*, The oncoprotein gankyrin binds to MDM2/HDM2, enhancing ubiquitylation and degradation of p53. *Cancer Cell*, 2005, **8**, 75–87.
8. Higashitsuji, H., Liu, Y., Mayer, R. J. and Fujita, J., The oncoprotein gankyrin negatively regulates both p53 and RB by enhancing proteasomal degradation. *Cell Cycle*, 2005, **4**, 1335–1337.
9. Nanaware, P. P., Ramteke, M. P., Somavarapu, A. K. and Venkatraman, P., Discovery of multiple interacting partners of gankyrin, a proteasomal chaperone and an oncoprotein – evidence for a common hot spot site at the interface and its functional relevance. *Proteins Struct. Funct. Bioinform.*, 2014, **82**, 1283–1300.
10. Sahu, I., Nanaware, P., Mane, M., Mulla, S. W., Roy, S. and Venkatraman, P., Role of a 19S proteasome subunit-PSMD10^{Gankyrin} in neurogenesis of human neural progenitor cells. *Int. J. Stem Cells*, 2019, **12**, 463–473.
11. Krzywdą, S. *et al.*, The crystal structure of Gankyrin, an oncoprotein found in complexes with cyclin-dependent kinase 4, a 19 S proteasomal ATPase regulator, and the tumor suppressors Rb and p53. *J. Biol. Chem.*, 2004, **279**, 1541–1545.
12. Nakamura, Y. *et al.*, Structure of the oncoprotein gankyrin in complex with S6 ATPase of the 26S proteasome. *Structure*, 2007, **15**, 179–189.

13. Modi, K., Dalvi, S. and Venkatraman, P., Two negatively charged invariant residues influence ligand binding and conformational dynamics of 14-3-3 ζ . *FEBS Lett.*, 2020, **594**, 878–886.
14. Winter, G., xia2: an expert system for macromolecular crystallography data reduction. *J. Appl. Crystallogr.*, 2010, **43**, 186–190.
15. Winn, M. D. *et al.*, Overview of the CCP4 suite and current developments. *Acta Crystallogr. Sect. D*, 2011, **67**, 235–242.
16. Liebschner, D. *et al.*, Macromolecular structure determination using X-rays, neutrons and electrons: recent developments in Phenix. *Acta Crystallogr. Sect. D*, 2019, **75**, 861–877.
17. Murshudov, G. N., Vagin, A. A. and Dodson, E. J., Refinement of macromolecular structures by the maximum-likelihood method. *Acta Crystallogr. Sect. D*, 1997, **53**, 240–255.
18. Emsley, P., Lohkamp, B., Scott, W. G. and Cowtan, K., Features and development of Coot. *Acta Crystallogr. Sect. D*, 2010, **66**, 486–501.
19. Pettersen, E. F. *et al.*, UCSF Chimera – a visualization system for exploratory research and analysis. *J. Comput. Chem.*, 2004, **25**, 1605–1612.
20. Schrödinger, LLC, The {PyMOL} Molecular Graphics System, Version 1.8, 2015.
21. Jumper, J. *et al.*, Highly accurate protein structure prediction with AlphaFold. *Nature*, 2021, **596**, 583–589.
22. Flower, T. G. and Hurley, J. H., Crystallographic molecular replacement using an *in silico*-generated search model of SARS-CoV-2 ORF8. *Protein Sci.*, 2021, **30**, 728–734.
23. Matthews, B. W., Solvent content of protein crystals. *J. Mol. Biol.*, 1968, **33**, 491–497.
24. Juers, D. H. and Ruffin, J., MAP-CHANNELS: a computation tool to aid in the visualization and characterization of solvent channels in macromolecular crystals. *J. Appl. Crystallogr. Sect.*, 2014, **47**, 2105–2108.
25. Li, J. *et al.*, Gankyrin, a biomarker for epithelial carcinogenesis, is overexpressed in human oral cancer. *Anticancer Res.*, 2011, **31**, 2683–2692.
26. Rickman, D. S. *et al.*, Prediction of future metastasis and molecular characterization of head and neck squamous-cell carcinoma based on transcriptome and genome analysis by microarrays. *Oncogene*, 2008, **27**, 6607–6622.
27. Zhen, C. *et al.*, Gankyrin promotes breast cancer cell metastasis by regulating Rac1 activity. *Oncogene*, 2012, **32**(29), 3452–3460.
28. Chattopadhyay, A. *et al.*, Discovery of a small-molecule binder of the oncoprotein gankyrin that modulates gankyrin activity in the cell. *Sci. Rep.*, 2016, **6**, 1–11.
29. Kanabar, D. *et al.*, Structural modification of the aryl sulfonate ester of cjoc42 for enhanced gankyrin binding and anti-cancer activity. *Bioorg. Med. Chem. Lett.*, 2020, **30**, 126889.
30. Mukund Sudharsan, M. G., Chikhale, R., Nanaware, P. P., Dalvi, S. and Venkatraman, P., A druggable pocket on PSMD10 Gankyrin that can accommodate an interface peptide and doxorubicin. *Eur. J. Pharmacol.*, 2022, **915**, 174718.
31. Müller, I., Guidelines for the successful generation of protein-ligand complex crystals. *Acta Crystallogr. Sect. D*, 2017, **73**, 79–92.
32. Serquera, D., Lee, W., Settanni, G., Marszalek, P. E., Paci, E. and Ltzhaki, L. S., Mechanical unfolding of an ankyrin repeat protein. *Biophys. J.*, 2010, 1294–1301.

ACKNOWLEDGEMENTS. Molecular graphics and analyses were performed with UCSF Chimera, developed by the Resource for Bio-computing, Visualization and Informatics at the University of California, San Francisco, USA with support from NIH P41-GM103311. We acknowledge use of the XRD facility of Advanced Centre for Treatment, Research and Education in Cancer (ACTREC) and Dr Gagandeep Gupta (BARC, Mumbai) for his suggestions. We also acknowledge the use of PX-BL21 beamline (BARC) at Indus-2, RRCAT, Indore and thank Dr M. V. Hosur (National Institute of Advanced Studies, Bengaluru) for useful discussions and guidance. M.S.M.G. thanks ACTREC for a fellowship.

Received 29 October 2021; revised accepted 12 January 2022

doi: 10.18520/cs/v122/i6/674-681